Preprint Title	Kinetically stabilized 1,3-diarylisobenzofurans and the possibility of preparing large, persistent isoacenofurans with unusually small HOMO-LUMO gaps
Authors	Qian Liu and Glen P. Miller
Publication Date	05 Dez. 2023
Article Type	Full Research Paper
Supporting Information File 1	Supporting Information (2).docx; 1.1 MB
ORCID® iDs	Glen P. Miller - https://orcid.org/0009-0004-7751-3573

Kinetically stabilized 1,3-diarylisobenzofurans and the possibility of preparing large, persistent isoacenofurans with unusually small HOMO-LUMO gaps

Qian Liu and Glen P. Miller[*]

Department of Chemistry, University of New Hampshire, Durham, NH USA

Abstract

We show that isoacenofurans of any size possess smaller HOMO-LUMO gaps than the corresponding acene bearing an isoelectronic π-system (i.e., the same total number of rings). Large isoacenofurans show limited stability due in part to the highly reactive 1,3-carbons of the furan ring. Placing sterically congesting phenyl substituents bearing *ortho* alkyl groups at the 1,3-positions of 1,3-diarylisobenzofurans force these molecules to adopt non-planar conformations with the *ortho* alkyl groups above and below the most reactive 1,3-carbons of the furan ring. These bulky substituents provide a strong measure of kinetic stabilization. Thus, 1,3-dimesitylisobenzofuran and 1,3-di(2',4',6'-triethylphenyl)isobenzofuran are at least 500 times less reactive than 1,3-diphenylisobenzofuran in their reactions with the strong dienophiles DMAD and acrylonitrile. The insights gained here suggest that the synthesis of large, persistent, kinetically stabilized isoacenofurans with unusually small HOMO-LUMO gaps is within reach. As such, these molecules deserve increased attention as potential p-type organic semiconductors.

Keywords

Isoacenofuran, Isobenzofuran, Isonaphthofuran, Isoanthracenofuran, Isotetracenofuran, Isopentacenofuran, 1,3-Diphenylisobenzofuran, 1,3-Dimesitylisobenzofuran, 1,3-Di(2',4',6'-triethylphenyl)isobenzofuran, 1,3-Di(2',4',6'-triisopropylphenyl)isobenzofuran, 1,3-Di(2',4',6'-tri-*t*-butylphenyl)isobenzofuran, Organic semiconductor, p-Type organic semiconductor, Acene, Small band-gap, Small HOMO-LUMO gap, Kinetically stabilized, Highly delocalized π-system, Sterically congesting substituent, Synthesis, DFT calculation

Introduction

Acenes are composed of linearly annellated benzene rings. Compared to their non-linearly annellated isomers, acenes possess smaller HOMO-LUMO gaps. This is attributed to their novel electronic structures which manifest that no more than one benzene ring can be drawn with a full aromatic sextet in any neutral, closed-shell resonance form (**Figure 1**).[1] One can view aromatic sextets in any one resonance form as π-electrons that are localized to one ring whereas other π-electrons are delocalized over the remaining π-system. Larger, delocalized π-systems are associated with smaller HOMO-LUMO gaps.

Isoacenofurans are composed of linearly annellated benzene rings that terminate with a furan ring. Isoacenofurans and acenes possess isoelectronic π-systems when the total number of rings is the same.

Compared to an acene, we expect an isoacenofuran with isoelectronic π-system to possess a more highly delocalized π-system and an even smaller HOMO-LUMO gap. This is because none of the benzene rings in an isoacenofuran possess an aromatic sextet in any neutral, closed-shell resonance form (**Figure 2**). For example, consider pentacene and isotetracenofuran. Pentacene can be drawn in several neutral, closed-shell resonance forms (**Figure 1**) in which any one of the five 6-membered rings possess an aromatic sextet. If the aromatic sextet is located in the first ring of the molecule, as in resonance forms P1 and P5 of **Figure 1**, then the remaining π-electrons are delocalized over a large area. However, calculations indicate that the center ring of pentacene and other acenes is the most aromatic[2] and therefore resonance form P3 of **Figure 1** is most significant.

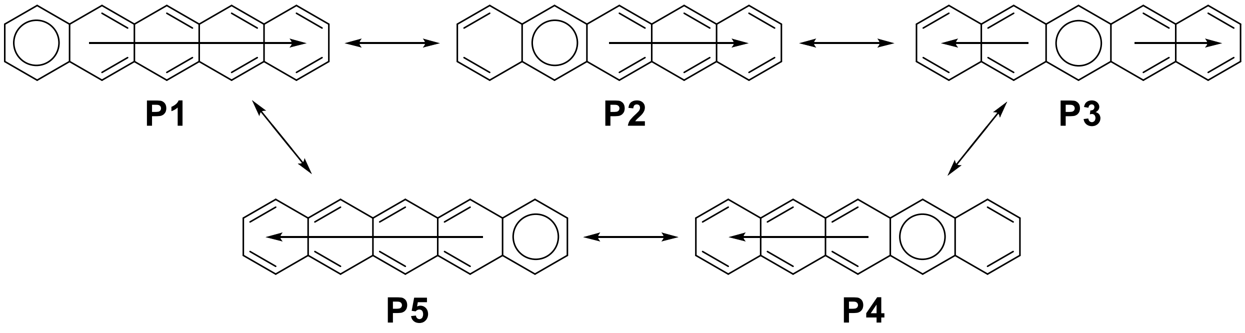

Figure 1. Neutral, closed-shell resonance forms for pentacene highlighting Clar aromatic sextets (see ref. 1) and the degree to which the remaining π-electrons are extensively delocalized, or not.

By contrast, isotetracenofuran and other isoacenofurans can only be drawn in one neutral, closed-shell resonance form in which only the furan ring possesses an aromatic sextet (**Figure 2**). Thus, compared to acenes, isoacenofurans possess a more highly delocalized π-system and are expected to exhibit smaller HOMO-LUMO gaps.

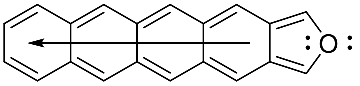

Figure 2. The only neutral, closed-shell resonance form for 5-ring isotetracenofuran with its highly delocalized π-system.

Hamura and co-workers pioneered the synthesis of large isoacenofurans. They prepared a pair of 1,3-diarylisoanthracenofurans[3] and a pair of 1,3-diphenethynylisoanthracenofurans,[4] and impressively utilized the latter as intermediates for the synthesis of stabilized hexacenes. Their beautiful work documented the lack of stability associated with isoanthraceneofurans. Thus, their 1,3-diarylisoanthracenofurans did not persist long in solution, rapidly forming endoperoxides.[3] These compounds persisted longer in the solid state, but clearly the lack of stability and persistence associated with isoacenofurans is of great concern if these molecules are to be utilized as organic semiconductors with unusually small HOMO-LUMO gaps. Likewise, Hamura and co-workers' 1,3-diphenethynylisobenzofurans were fleeting intermediates that could not be isolated, but were instead trapped *in situ* by suitable dienophile.[4]

Large acenes are prone to photooxidation, especially when dissolved in solution while exposed to ambient light and air. Large acenes are known to sensitize singlet oxygen formation, and the same is expected from large isoacenofurans. Indeed, the endoperoxides observed by Hamura and co-workers[3] confirm this expectation. We previously studied substituent effects in acenes and reported that several substituents promote photooxidative resistance in pentacenes[5] and larger acenes including heptacene[6] and nonacene.[7] One or more substituents that promote photooxidative resistance by quenching singlet oxygen could be utilized on isoacenofurans, too. Additionally, the 1,3-carbons of the furan ring in isoacenofurans are highly reactive towards dienophiles, including singlet oxygen. Thus, the design of large, persistent isoaceneofurans should include multiple substituents that provide both photooxidative resistance, especially along the acene-like segment, and a strong measure of kinetic stabilization at the 1,3-carbons of the furan ring.

In this work, we report computational HOMO-LUMO gaps associated with isoacenofurans and compare them to the HOMO-LUMO gaps of acenes with the same total number of rings (isoelectronic π-systems). The data provides compelling reasons to contemplate the synthesis of large, persistent isoacenofurans as p-type organic semiconductors. Experimentally, we synthesized two 1,3-diarylisobenzofurans that provide steric resistance to the most reactive 1,3-carbons of the furan ring. A combination of experimental and computational studies clarify the impacts of these sterically congesting substituents on each molecule's electronic structure. We further studied the reaction rates of 1,3-diarylisobenzofurans with the strong dienophiles dimethyl acetelyenedicarboxylate (DMAD) and acrylonitrile. We conclude that the synthesis of large, persistent, kinetically stabilized isoacenofurans with unusually small HOMO-LUMO gaps is within reach.

Results and Discussion

1. Computational HOMO-LUMO gaps for isoacenofurans and comparable acenes

We studied the HOMO-LUMO gaps associated with acenes and isoacenofurans (**Table 1**) using a DFT method that has proven reliable for large acenes both in terms of absolute values and trends. In all cases, isoacenofurans possess a smaller HOMO-LUMO gap than the corresponding acene with an isoelectronic π-system. For example, naphthalene and isobenzofuran, **1**, both possess 10 π-electrons and are calculated to have HOMO-LUMO gaps of 4.73 and 4.05 eV, respectively. The incorporation of 1,3-diphenyl substituents (compound **2**) or 1,3-diphenylthio substituents (compound **4**) lowers the HOMO-LUMO gaps of the corresponding isobenzofurans to 3.05 and 3.65 eV, respectively. These groups provide for expanded delocalization of π-electron density outside the isobenzofuran core. Phenylthio substituents have also been shown to impart considerable photooxidative resistance to pentacene.[5] The incorporation of 1,3-dimesityl substituents (compound **3**) also provides for modest lowering of the HOMO-LUMO gap despite the non-planar geometry that these groups must adopt (**Figure 3**). We are keenly interested in preparing isoacenofurans with small HOMO-LUMO gaps. The non-planar geometry of mesityl and similar groups additionally provides for enhanced steric congestion at the most reactive 1,3-carbons of the furan ring (vide infra), and this could prove to be an important design strategy for large, persistent isoacenofurans.

The trend continues for the entire acene series calculated, from anthracene to hexacene (**Table 1**). Thus, pentacene, a benchmark organic semiconductor, has a calculated HOMO-LUMO gap is 2.18 eV, nearly 0.5 eV greater than that of isotetracenofuran, **13**, with an isoelectronic π–system (22 π-electrons each). The incorporation of 1,3-diphenyltio groups (compound **16**) slightly lowers the HOMO-LUMO gap to 1.65 eV. Even in the presence of sterically congesting, non-planar 1,3-dimesityl groups, the corresponding isotetracenofuran, **15**, possesses an unusually small HOMO-LUMO gap of 1.59 eV. Among the isoacenofurans studied here, the smallest calculated HOMO-LUMO gaps are observed in the isopentacenofuran series (compounds **17**-**20**). They possess HOMO-LUMO gaps just north of 1.2 eV.

These Spartan '20[9] calculations confirm our expectation of a more highly delocalized π-system in any isoacenofuran (**Figure 2**) compared to the corresponding acene with isoelectronic π-system (**Figure 1**). As such, isoacenofurans represent a highly interesting class of molecules that, although largely ignored in the literature, deserve increased attention as potential p-type organic semiconductors with unusually small HOMO-LUMO gaps.

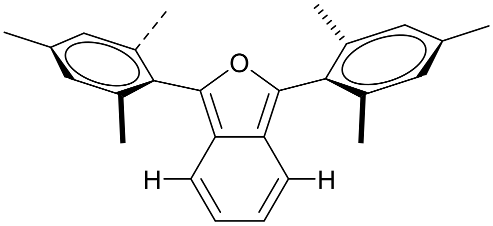

Figure 3. A structural rendering of 1,3-dimesitylisobenzofuran showing the requirement for non-planar mesityl groups in order to avoid steric repulsion between *ortho*-methyl groups and the nearest benzo hydrogen atoms

2. Synthesis of two 1,3-diarylisobenzofurans with sterically congesting substituents

In order to study the impacts of sterically congesting substituents at the 1,3-carbons of the furan ring, we synthesized two 1,3-diarylisobenzofurans (compounds **3** and **23**, **Scheme 1**). Combined with commercially available **2**, these compounds provide varying degrees of steric congestion to the most highly reactive 1,3-carbons on the furan ring. Thus, phthaloyl chloride was reacted with mesitylene or 1,3,5-triethylbenzene to produce the corresponding diketones, **21** and **22**. Each diketone was in turn reacted with zinc metal in glacial acetic acid[8] to afford the corresponding 1,3-diarylisobenzofurans, **3** and

Table 1. DFT calculated HOMO-LUMO gaps of acenes and isoacenofurans performed at the B3LYP/6-311+G(d,p)//B3LYP/6-31G(d) level of theory using Spartan '20[9]

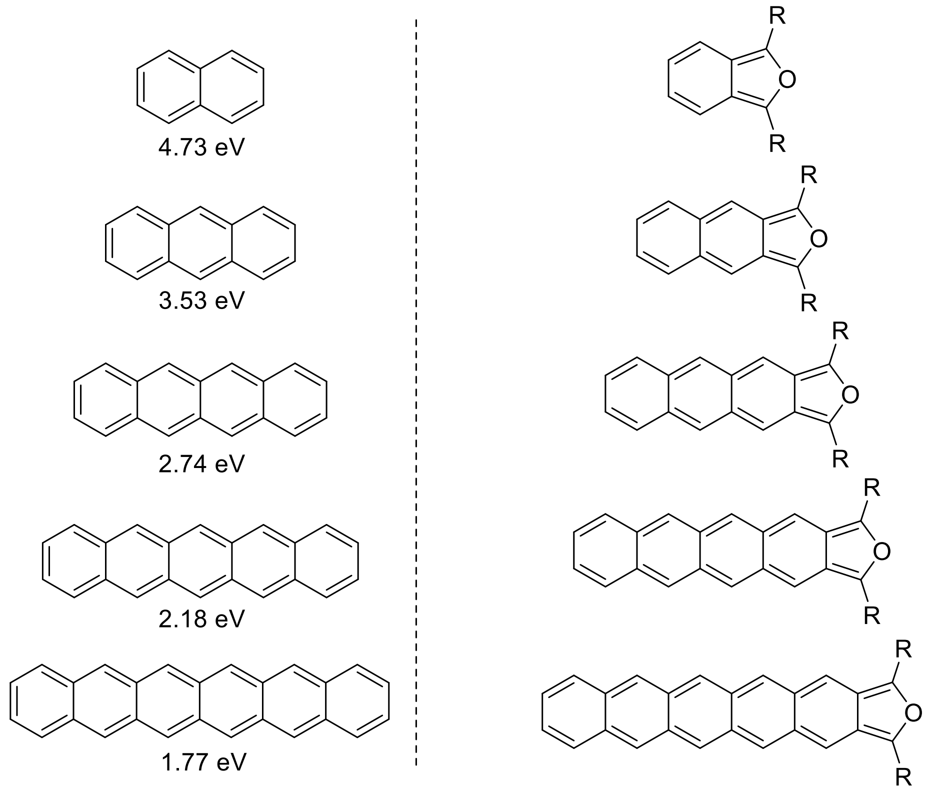

1	R = H	4.05 eV
2	R = Ph	3.05 eV
3	R = Mesityl	3.57 eV
4	R = SPh	3.65 eV
5	R = H	2.89 eV
6	R = Ph	2.36 eV
7	R = Mesityl	2.63 eV
8	R = SPh	2.73 eV
9	R = H	2.17 eV
10	R = Ph	1.86 eV
11	R = Mesityl	2.01 eV
12	R = SPh	2.09 eV
13	R = H	1.69 eV
14	R = Ph	1.51 eV
15	R = Mesityl	1.59 eV
16	R = SPh	1.65 eV
17	R = H	1.36 eV
18	R = Ph	1.25 eV
19	R = Mesityl	1.28 eV
20	R = SPh	1.34 eV

Scheme 1. Synthesis of 1,3-diarylisobenzofurans **3** and **23**

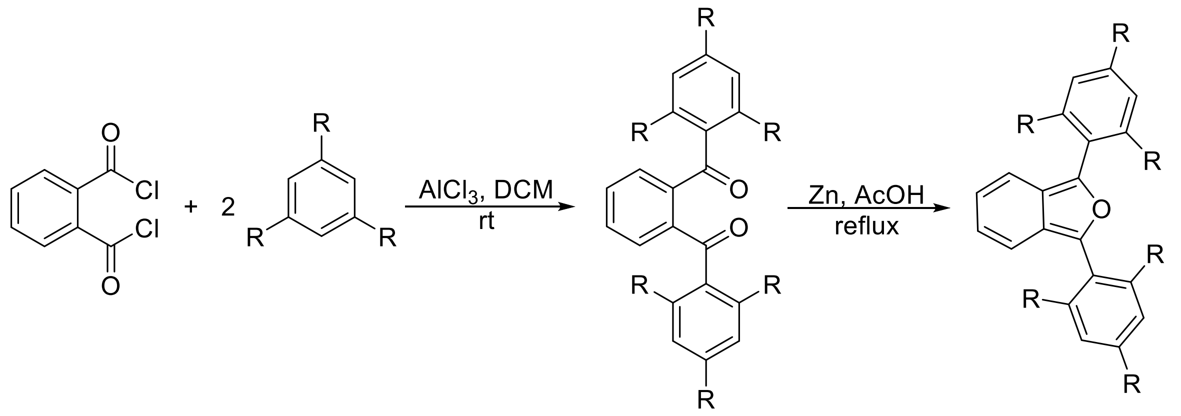

21 R = Me 99%
22 R = Et 35%

3 R = Me 60%
23 R = Et 62%

23. The latter reductions in the presence of zinc likely proceed through the corresponding ketols which are known to undergo ring closure in acidic solution.[10] These syntheses utilizing mesitylene or 1,3,5-triethylbenzene are considerably simpler than other approaches that would place sterically congesting groups only at the *ortho* positions of the 1,3-diaryl substituents. Compounds **3** and **23** contain an additional *para* substituent that serves no particular purpose but is innocuous.

The syntheses of compounds **24** and **25** with 2',4',6'-triisopropylphenyl and 2',4',6'-tri-*t*-butylphenyl substituents, respectively, were also attempted but without success. In these cases, the sterically congesting *ortho* isopropyl and *t*-butyl groups stymie the Friedel-Crafts acylation step leading to diketone (**Scheme 1**).

3. Experimental and computational studies of 1,3-diarylisoacenofurans

Purified isobenzofurans **2**, **3** and **23** were studied by UV-vis and fluorescence spectroscopies (**Figure 4**). Compound **2** is devoid of *ortho* groups on its 1,3-diphenyl substituents and shows the longest wavelengths of absorption (λ_{max} = 415 nm) and emission (emission λ_{max} = 484 nm) in this series, consistent with a more highly conjugated π-system in which the 1,3-diphenyl substituents lie flat or nearly flat relative to the isobenzofuran backbone. Likewise, compound **2** is yellow while compounds **3** and **23** are colorless. Compounds **3** and **23** show similar absorption (λ_{max} = 364 and 360 nm for **3** and **23**, respectively) and emission (λ_{max} = 442 and 436 nm for **3** and **23**, respectively) spectra, both consistent with a less conjugated π-system compared to **2**. This is due entirely to out-of-plane rotation of the sterically congesting 1,3-diaryl groups (**Figure 3**).

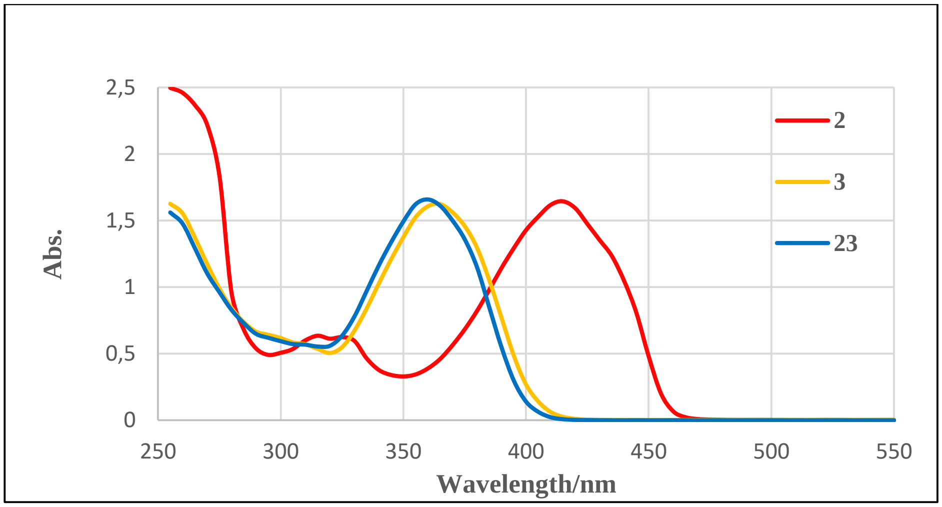

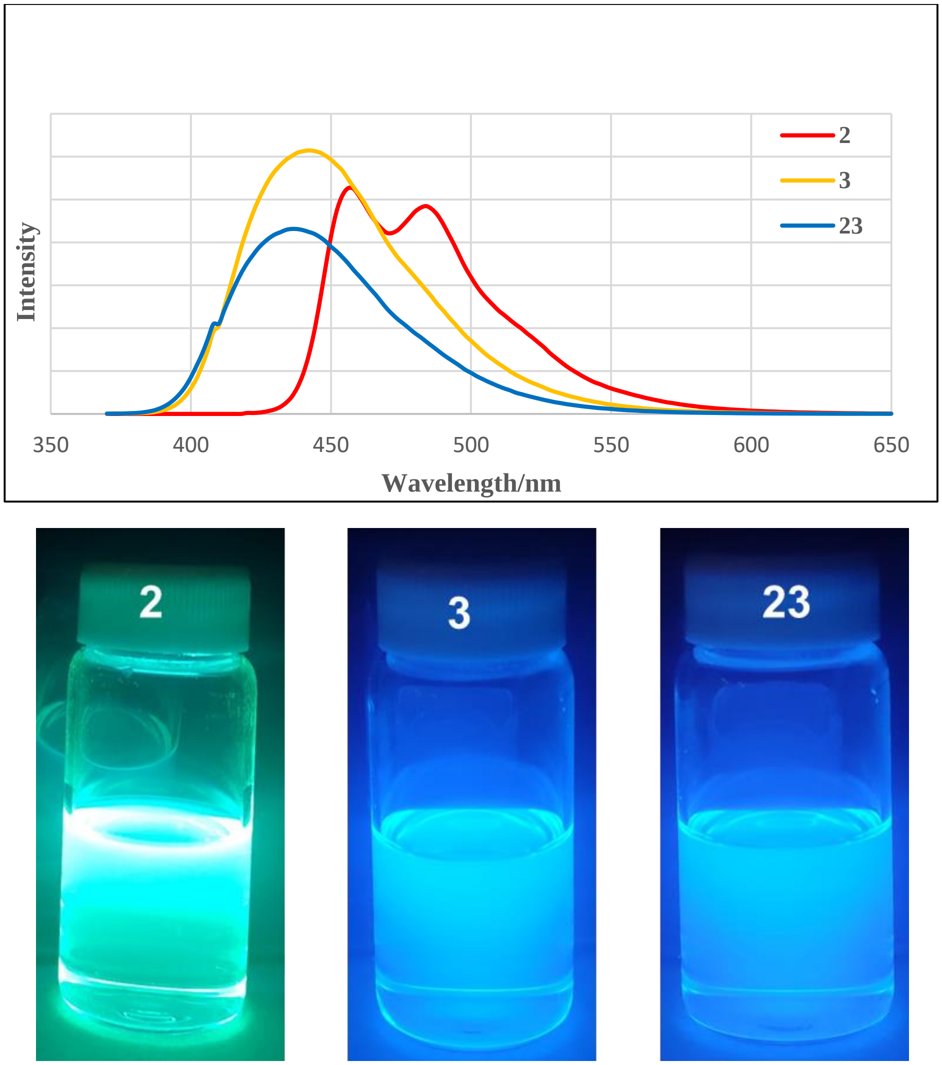

Figure 4. UV-vis (top) and fluorescence (bottom) spectra for 10^{-6} M solutions of 1,3-diarylisobenzofurans **2**, **3** and **23** in CH_2Cl_2 solvent. The vials of **2**, **3** and **23** showing fluorescence emission (bottom) were excited at 365 nm.

In order to further probe the impact of sterically congesting 1,3-diaryl substituents in 1,3-diarylisobenzofurans, we studied compounds **1**, **2**, **3**, **23**, **24** and **25** (**Figure 5**) using a DFT method. The calculated HOMO and LUMO orbitals are shown in **Figure 5**. Here, the impacts of 1,3-diaryl substituents are illuminated. Thus, both HOMO and LUMO orbital densities for **2** are spread throughout the molecule's entire π-system including the 1,3-diphenyl substituents. This extensive delocalization of orbital density significantly raises the HOMO energy level and lowers the LUMO energy level compared to parent isobenzofuran **1**. Conversely, both the HOMO and LUMO orbitals for compound **3** with 1,3-dimesityl substituents show reduced orbital density on the mesityl substituents compared to the phenyl substituents of **2**. Likewise, **3** possesses a lower energy HOMO orbital and a higher energy LUMO orbital compared to **2**. The π-systems for compounds **23**, **24** and **25** with 2',4',6'-triethylphenyl, 2',4',6'-

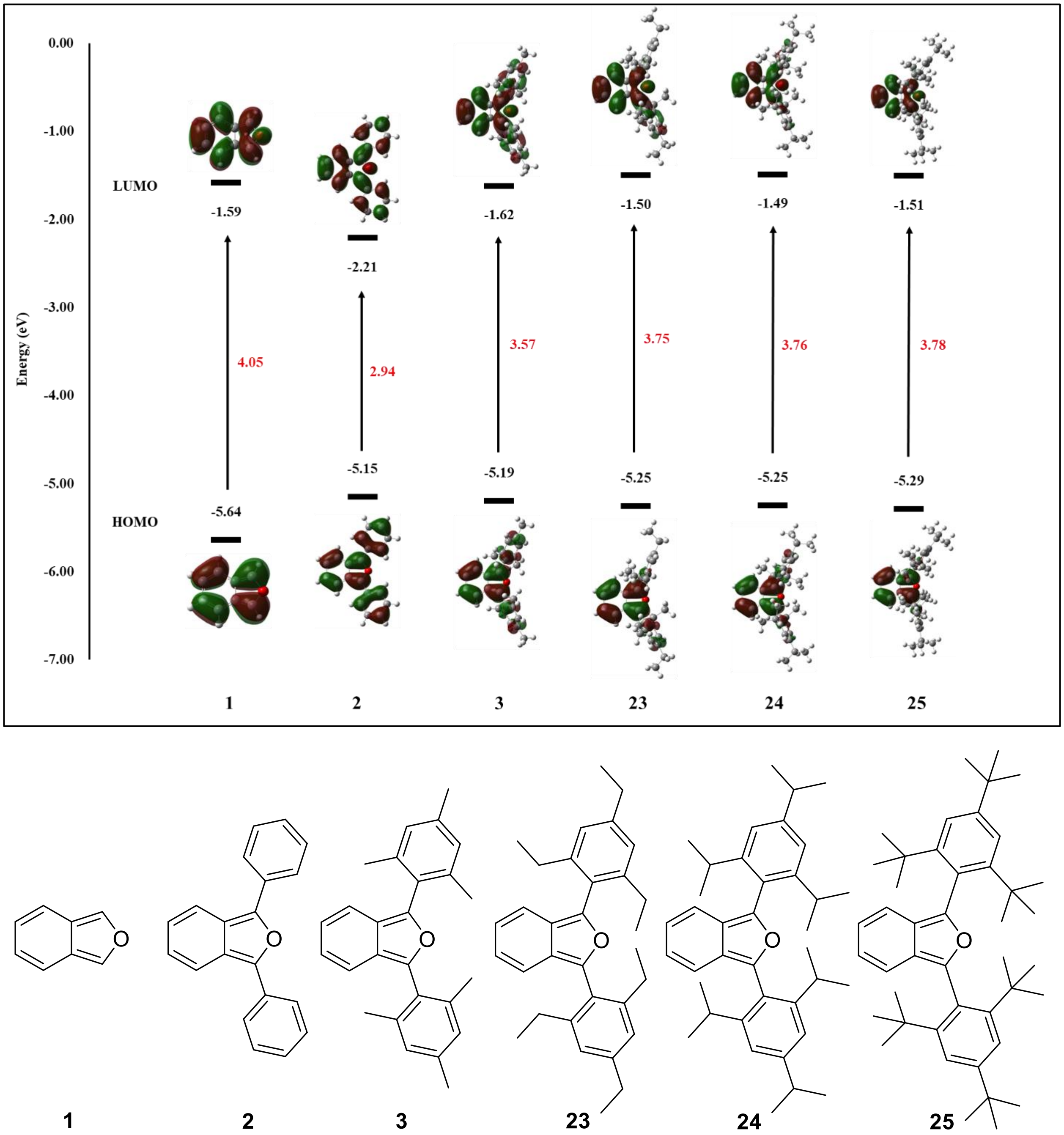

1 **2** **3** **23** **24** **25**

Figure 5. Calculated HOMO and LUMO orbitals for parent isobenzofuran **1** and 1,3-diarylisobenzofuran derivatives **2**, **3**, **23**, **24** and **25** using a DFT method performed at the B3YLP/6-311+G(d,p)//B3YLP/6-31G(d) level using Gaussian 09[11]

triisopropylphenyl and 2',4',6'-tri-*t*-butylphenyl substituents are quite similar to each other. Each shows little or no HOMO or LUMO orbital densities on their respective 1,3-diaryl groups indicating greater out-of-plane rotation compared to **3** and modestly larger HOMO-LUMO gaps.

The calculated UV-vis spectra for this series are shown in **Figure 6**. Compounds **23**, **24** and **25** show nearly identical spectra indicating that each hindered 1,3-diaryl ring is similarly rotated out of plane leading to π-systems with similar HOMO-LUMO gaps. Unless there is a need for improved kinetic stabilization of the most reactive 1,3-carbons on the furan ring, there appears little benefit of utilizing highly hindered 2',4',6'-triisopropyl (compound **24**) or 2',4',6'-tri-*t*-butyl (compound **25**) substituents, especially as these compounds are considerably more difficult to synthesize compared to **3** and **23**.

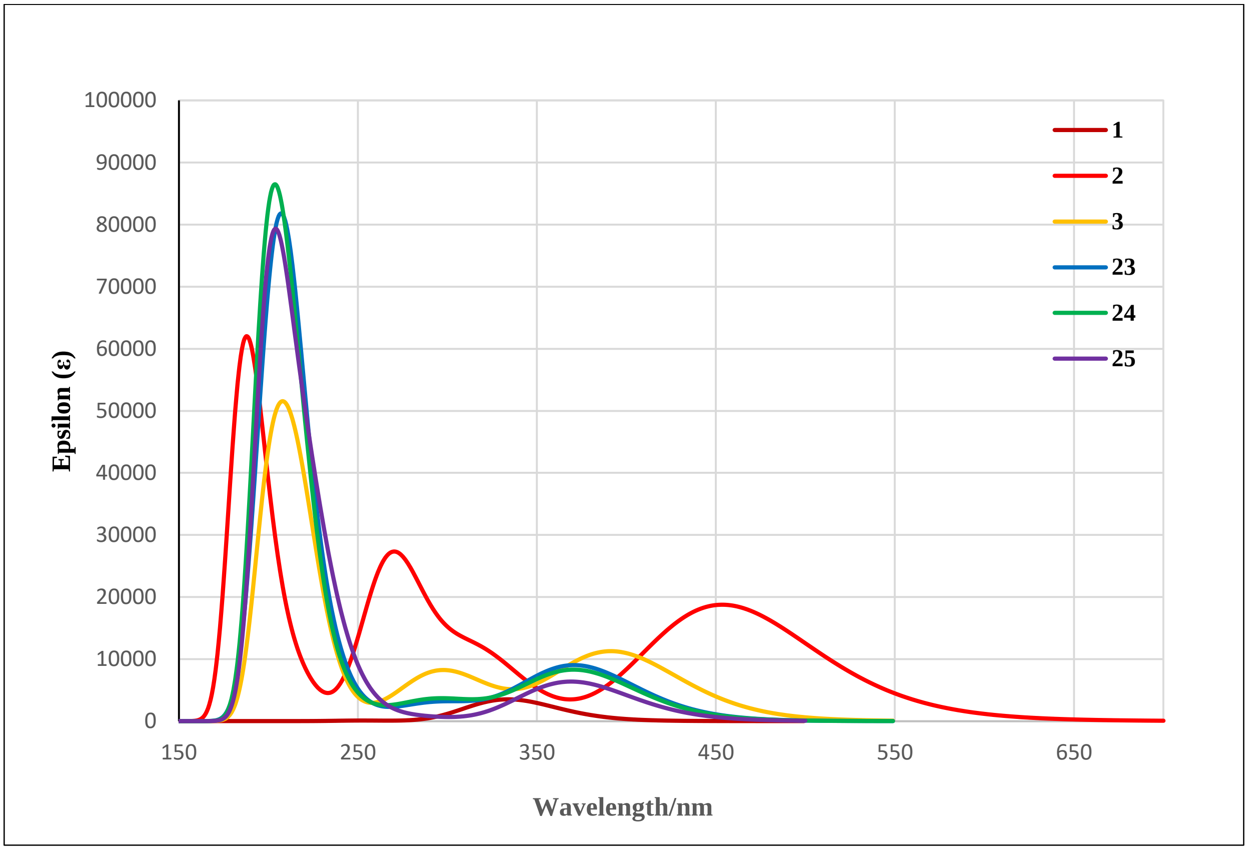

Figure 6. UV-vis spectra calculated for 1,3-diarylisobenzofuran derivatives **1**, **2**, **3**, **23**, **24** and **25** using a DFT method performed at the B3YLP/6-311+G(d,p)//B3YLP/6-31G(d) level using Gaussian 09[11]

4. Relative rates for the reactions between 1,3-diarylisobenzofurans 2, 3 and 23 with the strong dienophiles dimethyl acetelyenedicarboxylate (DMAD) and acrylonitrile

We studied the reactions of **2**, **3** and **23** under pseudo-1st order kinetic conditions by utilizing a 7000-fold excess of dimethyl acetylenedicarboxylate (DMAD) at room temperature. The reactions were monitored by UV-vis spectroscopy. Compound **2** undergoes relatively rapid reaction with DMAD under these conditions and is more than 90% consumed after 2.5 hours (**Figure 7a**). Conversely, compounds **3** (**Figure 7b**) and **23** are unreactive under these conditions, even after extended periods of time. The absorptions for **3** and **23** actually increased slowly over extended time due to the gradual evaporation of CH_2Cl_2 solvent in the capped UV-vis cuvette. Similar results were obtained upon switching the dienophile from DMAD to acrylonitrile. Once again, compounds **3** and **23** were unreactive, even after 184 hours of reaction time with a 13,500-fold excess of acrylonitrile (**Figure 7c**).

The reaction between **3** and a large excess of DMAD (116 equivalents) in boiling CH_2Cl_2 (39.6 °C) was also studied by ^{1}H NMR spectroscopy. After 51 hours of reaction in boiling CH_2Cl_2, Diels-Alder adduct **27** was

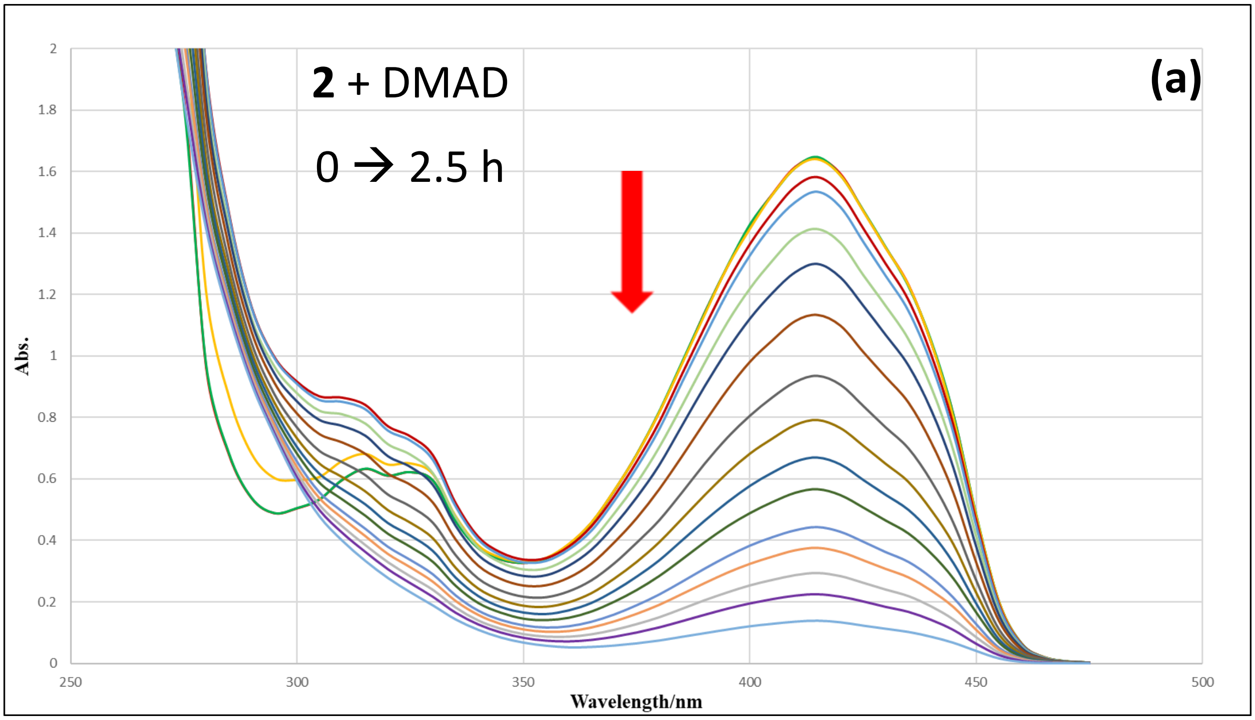

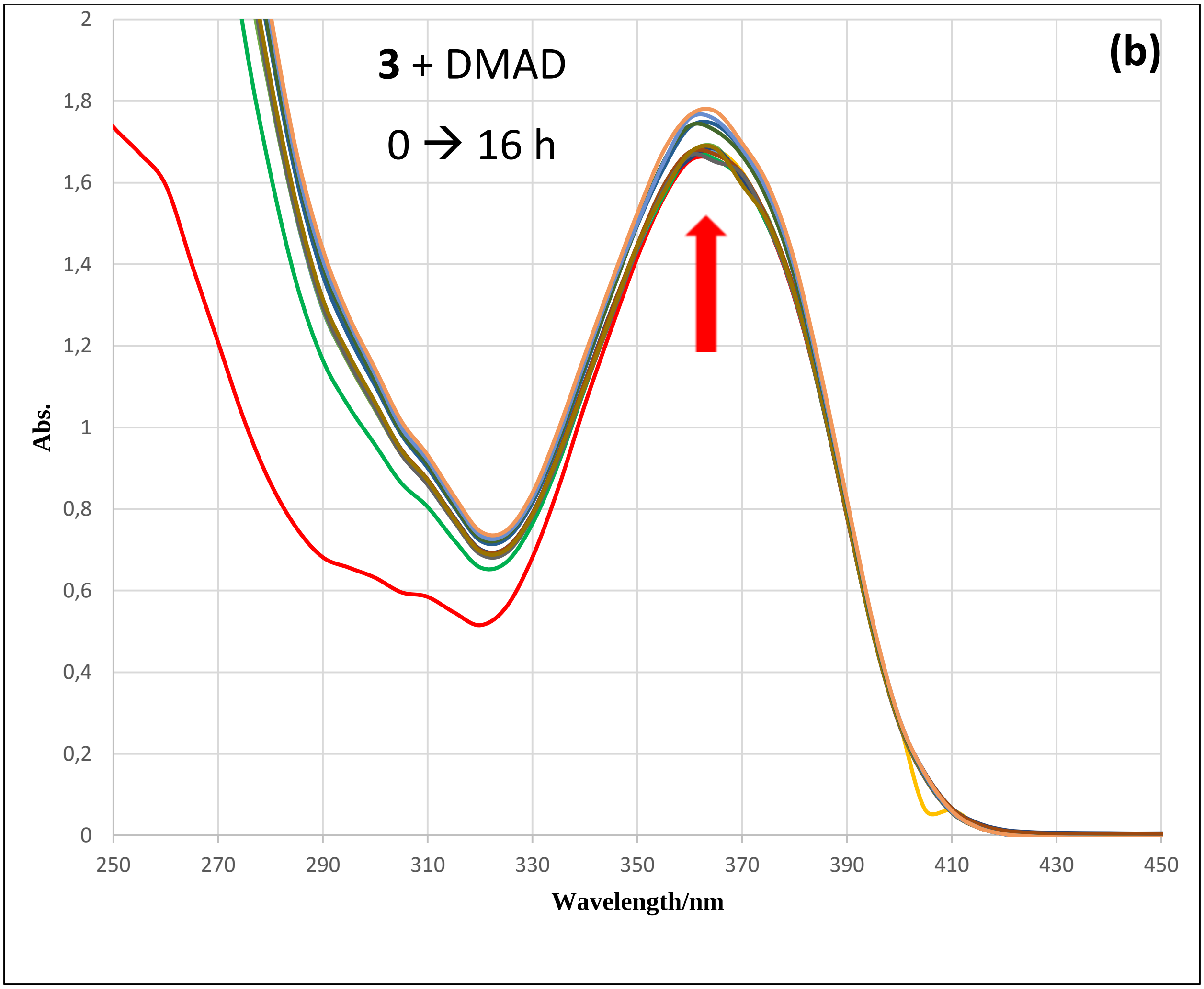
3 + DMAD
0 → 16 h
(b)
Abs.
2
1,8
1,6
1,4
1,2
1
0,8
0,6
0,4
0,2
0
250
270
290
310
330
350
370
390
410
430
450
Wavelength/nm

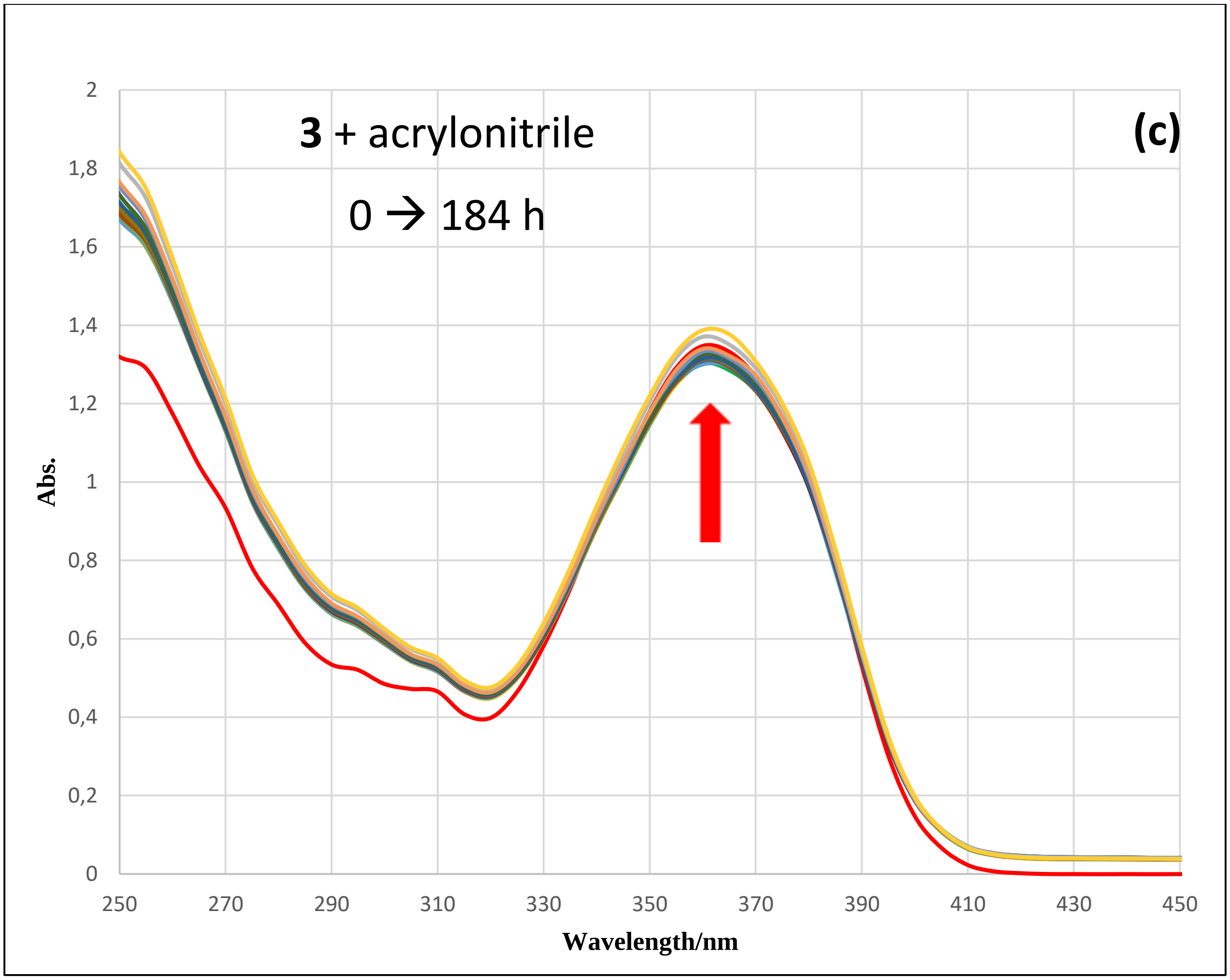

Figure 7. UV-vis spectra for the reactions of **2** (a) and **3** (b) with a 7000-fold excess of DMAD in CH_2Cl_2 solvent at room temperature, and for the reaction of **3** with 13,500-fold excess of acrylonitrile (c) in CH_2Cl_2 solvent at room temperature.

observed in 22% yield. Compound **27** was identified by ^{1}H NMR and ^{13}C NMR spectroscopies as well as high-resolution ESI mass spectrometry.

Although the lack of reactivity observed for **2** and **23** limited our kinetic analysis, we can nonetheless conclude that the rates of reactions between either **3** or **23** and either of the strong dienophiles, DMAD or acrylonitrile, are at least 500 times slower than the corresponding reactions involving **2** (**Scheme 2**). Clearly, the non-planar geometry of the mesityl (**Figure 3**) and 2’,4’,6’-triethylphenyl substituents in compounds **3** and **23**, respectively, provides for enhanced steric congestion at the most reactive 1,3-carbons of the furan ring. Likewise, **3** and **23** are stable indefinitely in the solid state (see Supporting

Information). The mesityl and 2',4',6'-triethylphenyl substituents both provide a strong measure of kinetic stabilization.

Scheme 2. Reactions between 1,3-diarylisobenzofurans **2**, **3** and **23** and DMAD to produce Diels-Alder adducts **26**, **27** and **28**

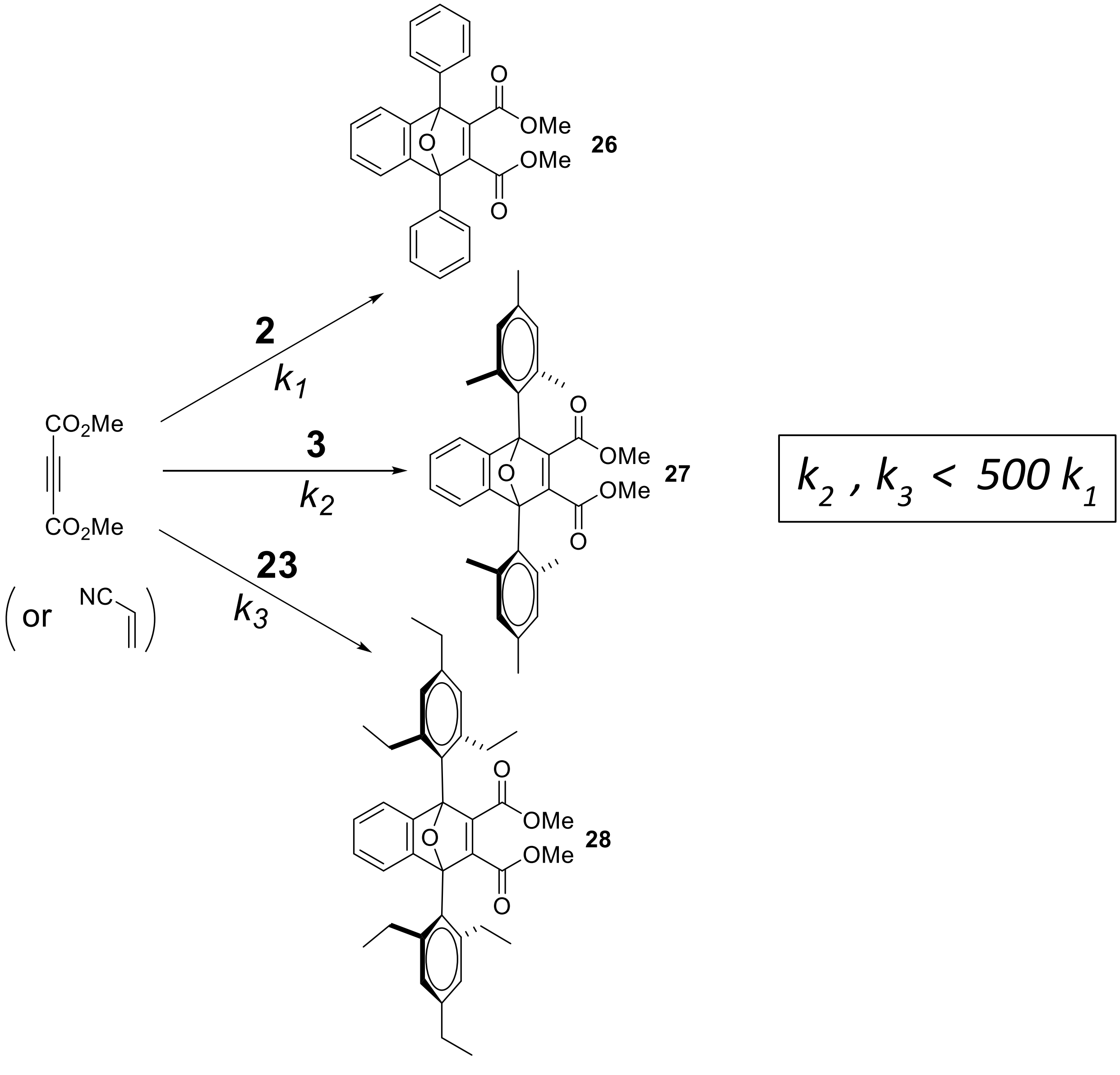

Conclusions

Isoacenofurans of any size possess smaller HOMO-LUMO gaps than the corresponding acene with an isoelectronic π-system, providing compelling reasons to design large, persistent isoacenofurans as p-type organic semiconductors. Sterically congesting *ortho* groups on 1,3-diarylisobenzofurans like **3** and **23** force these molecules to adopt non-planar conformations in which the aryl groups rotate out-of-plane. Due to these non-planar conformations, the HOMO and LUMO orbitals for **3** and **23** and related compounds show reduced orbital densities on their aryl substituents, effectively reducing π-conjugation and raising HOMO-LUMO gaps. The non-planar geometries of the mesityl and 2′,4′,6′-triethylphenyl substituents in compounds **3** and **23**, respectively, provide for enhanced steric congestion above and below the most reactive 1,3-carbons of the furan ring, dramatically reducing their reactivity with dienophiles. These bulky substituents provide a strong measure of kinetic stabilization. Compounds **3** and **23** are at least 500 times less reactive than **2** with the strong dienophiles DMAD and acrylonitrile. There appears little benefit to utilizing highly hindered 2′,4′,6′-triisopropylphenyl groups as in **24** or 2′,4′,6′-tri-*t*-butylphenyl groups as in **25**, especially as (i) isoacenofurans with these substituents are considerably more difficult to synthesize, and (ii) compounds **3** and **23** already provide excellent kinetic stabilization to the most reactive 1,3-carbons of the furan ring. Like acenes, large isoacenofurans will be prone to photooxidation, necessitating additional, strategically placed substituents that are known to quench singlet oxygen. The insights gained here suggest that the synthesis of large, persistent, kinetically stabilized isoacenofurans with unusually small HOMO-LUMO gaps is within reach. As such, these molecules deserve increased attention as potential p-type organic semiconductors.

Data Availability Statement

Supporting Information is available and includes ^{1}H and ^{13}C NMR spectra of key compounds plus high-resolution mass spectra for new compounds

Experimental

Materials and Methods:

Commercial reagents and solvents were purchased from Sigma Aldrich, Alfa Aesar, TCI America or Thermo Fisher Scientific Chemicals, and used as received. Dry solvents were obtained using a solvent purification system (Innovative Technologies, Inc.) and handled under a nitrogen atmosphere, unless otherwise noted. Flash chromatography was performed using SiliaFlash® F60 40-63 µm (230-400 mesh) 60 Å silica from Silicycle Inc. and RediSep® Rf Silica Flash Columns (12 g, 24 g or 40 g) on a CombiFlash® Rf 200 instrument (Teledyne Isco, Inc.). Evaporation of solvents was accomplished using an IKA® RV 10 digital rotary evaporator. Baker-flex® silica gel IB2-F thin layer chromatography (TLC) plates were purchased from J.T. Baker. A 4-watt 254 nm lamp (Analtytik Jena Co.) and a modified cardboard box were utilized for detection of TLC spots. Melting points were determined in open capillary tubes using a Mel-Temp apparatus, and are uncorrected. Proton nuclear magnetic resonance (^{1}H NMR) spectra and carbon nuclear magnetic resonance (^{13}C NMR) spectra were recorded on either a Bruker 500 MHz or Bruker 700 MHz Nuclear Magnetic Resonance Spectrometer using 5 mm NMR tubes with plastic caps. High-resolution mass spectra (HRMS) were obtained on a Thermo Scientific Vanquish UHPLC and Exploris 120 Mass Spectrometer at at the University of New Hampshire's University Instrumentation Center using a peak-matching protocol to determine the mass and error range of the molecular ion, and employing electrospray as the ionization technique. UV-Vis absorption spectra were measured with a Varian Cary 50 Scan UV-Visible Spectrophotometer and corrected for background signal with a solvent-filled cuvette. Fluorescence spectra were measured on FS5 Spectrofluorometer (150 W CW Ozone-free xenon arc lamp) from Edinburgh Instruments.

1,3-Dimesitylisobenzofuran (**3**):

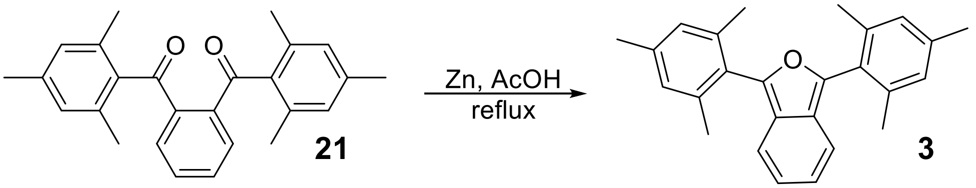

To a round bottom flask was added 1,2-phenylenebis(mesitylmethanone), **21** (0.10 g, 0.27 mmol), zinc dust (0.70 g, 10.80 mmol) and 10 mL glacial acetic acid. After attaching a reflux condenser, the mixture was heated to reflux for 12 hours with stirring. The hot reaction solution was filtered. To the hot filtrate was added 5 mL of cold water leading to the precipitation of crude product. The crude product was vacuum filtered, washed with 5 mL water, and then air dried to give **3** as a white solid. (57 mg, 60%). M.p. 169-170 °C. ^{1}H NMR (500 MHz, $CDCl_3$) δ 7.15 – 7.08 (m, 2H), 6.98 (s, 4H), 6.86 – 6.79 (m, 2H), 2.35 (s, 6H), 2.12 (s, 12H). ^{13}C NMR (126 MHz, $CDCl_3$) δ 143.54, 139.17, 138.71, 128.23, 127.43, 123.39, 121.93, 119.78, 21.22, 20.49. UV-Vis λ_{max} (7×10^{-5} M in CH_2Cl_2) 364.3 nm. HRMS (ESI): 355.2042 [calc'd for $M+H^+$: 355.2062].

1,2-Phenylenebis(mesitylmethanone) (**21**):

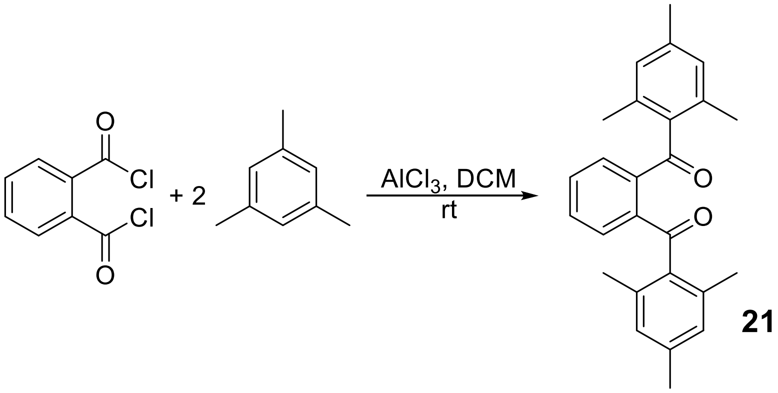

To a 100 mL round bottom flask equipped with a stir bar was added anhydrous aluminum chloride (0.26 g, 1.97 mmol) and 10 mL of CH_2Cl_2 solvent. An additional funnel was attached and to this was added phthaloyl dichloride (0.20 g, 0.99 mmol) and 5 mL CH_2Cl_2. The contents of the additional funnel were added dropwise into the round bottom flask over 5 minutes with stirring. The addition funnel was reloaded with mesitylene (0.215g, 1.79 mmol) and an additional 5 mL CH_2Cl_2. The contents of the additional funnel were once again added dropwise into the round bottom flask over 5 minutes with stirring. The light-yellow solution turned to dark brown. After 15 min, 10 mL of a saturated aqueous solution of NaCl was added to quench the reaction. The contents of the flask were transferred to a 125 mL separatory funnel and extracted twice with 20 mL of CH_2Cl_2. The organic extracts were combined, dried over anhydrous Na_2SO_4 and gravity filtered. The solvent was evaporated at reduced pressure leaving a yellow solid as crude product. The crude product was recrystallized using 10 mL of hexane to obtain **21** as a crystalline white solid (0.33g, 99%). M.p. 234-235 °C. ^{1}H NMR (500 MHz, $CDCl_3$) δ 7.48 – 7.36 (m, 4H), 6.86 (s, 4H), 2.30 (s, 6H), 2.19 (s, 12H). ^{13}C NMR (126 MHz, $CDCl_3$) δ 199.60, 141.23, 139.54, 136.54, 136.07, 131.22, 130.38, 129.00, 21.17, 20.29.

1,2-Phenylenebis((2,4,6-triethylphenyl)methanone) (**22**):

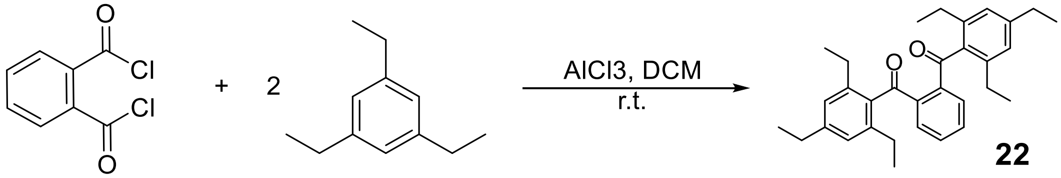

To a 100 mL round bottom flask equipped with a stir bar was added anhydrous aluminum chloride (0.66 g, 4.93 mmol) and 10 mL of CH_2Cl_2 solvent. An additional funnel was attached and to this was added phthaloyl dichloride (0.56 g, 2.76 mmol) and 5 mL CH_2Cl_2. The contents of the additional funnel were added dropwise into the round bottom flask over 5 minutes with stirring. The addition funnel was reloaded with 1,3,5-triethylbenzene (0.9 g, 5.52 mmol) and an additional 5 mL CH_2Cl_2. The contents of the additional funnel were once again added dropwise into the round bottom flask over 5 minutes with stirring. The light-yellow solution turned to dark brown. After 30 min, 10 mL of a saturated aqueous solution of NaCl was added to quench the reaction. The contents of the flask were transferred to a 125 mL separatory funnel and extracted twice with 20 mL of CH_2Cl_2. The organic extracts were combined, dried over anhydrous Na_2SO_4 and gravity filtered. The solvent was evaporated at reduced pressure leaving a yellow oil. The oil was purified by silica gel CombiFlash chromatography (hexane/EtOAc = 9/1) to obtain **22** as a yellow solid (0.44 g, 35%). M.p. 59-60 °C. ^{1}H NMR (500 MHz, $CDCl_3$) δ 7.43 (s, 4H), 6.93 (s, 4H), 2.64 (q, *J* = 7.6 Hz, 4H), 2.53 (q, *J* = 7.5 Hz, 8H), 1.25 (t, *J* = 7.6 Hz, 6H), 1.08 (t, *J* = 7.5 Hz, 12H). ^{13}C NMR (126 MHz, $CDCl_3$) δ 199.43, 145.73, 142.40, 141.03, 135.73, 131.19, 131.05, 125.93, 28.78, 26.50, 15.81, 15.34. HRMS (ESI): 455.2938 [calc'd for M+H$^+$: 455.2950].

1,3-Bis(2,4,6-triethylphenyl)isobenzofuran (**23**):

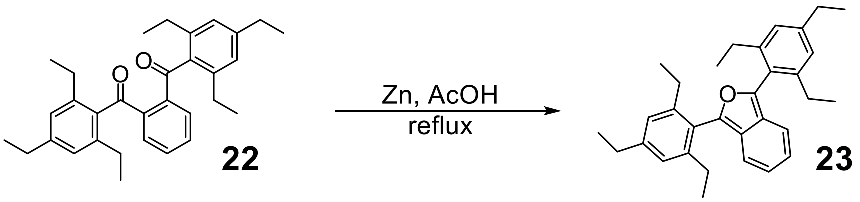

To a round bottom flask was added 1,2-phenylenebis((2,4,6-triethylphenyl)methanone), **22** (0.2 g, 0.44 mmol), zinc dust (1.15 g, 17.6 mmol) and 13 mL glacial acetic acid. After attaching a reflux condenser, the mixture was heated to reflux for 12 hours with stirring. The hot reaction solution was filtered. To the hot filtrate was added 5 mL of cold water leading to precipitation of crude product. The crude product was vacuum filtered, washed with 5 mL water, and then air dried to give **23** as a white solid (0.12 g, 62%).

M.p. 83-84 °C. ^{1}H NMR (500 MHz, CDCl$_3$) δ 7.15 – 7.08 (m, 2H), 7.02 (s, 4H), 6.84 – 6.77 (m, 2H), 2.69 (q, *J* = 7.6 Hz, 4H), 2.44 (qd, *J* = 5.2, 7.3 Hz, 8H), 1.30 (t, *J* = 7.6 Hz, 6H), 1.01 (t, *J* = 7.5 Hz, 12H). ^{13}C NMR (126 MHz, CDCl$_3$) δ 145.90, 145.48, 143.28, 126.29, 125.50, 123.32, 122.18, 119.64, 28.85, 27.14, 15.82, 15.37. UV-Vis λ_{max} (7×10^{-5} M in CH$_2$Cl$_2$) 360.2 nm. HRMS (ESI): 439.2987 [calc'd for M+H$^+$: 439.3001].

Dimethyl 1,4-diphenyl-1,4-dihydro-1,4-epoxynaphthalene-2,3-dicarboxylate (**26**):

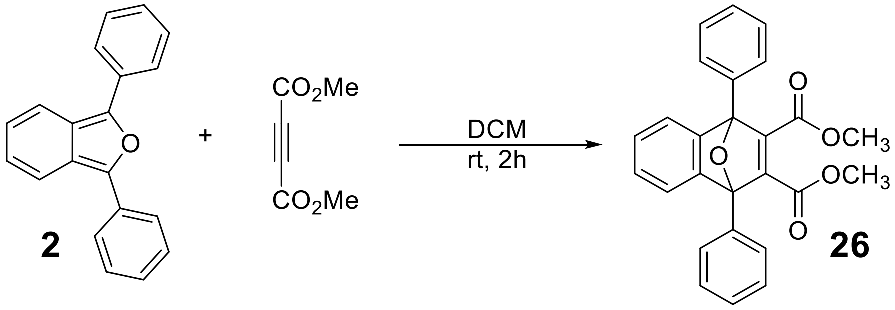

To a round bottom flask was added 1,3-diphenylisobenozfuran, **2** (0.100 g, 0.37 mmol), 5 mL CH$_2$Cl$_2$ and dimethyl acetylenedicarboxylate (DMAD, 0.116 g, 0.814 mmol). The reaction mixture was stirred at room temperature for 2 hours. The solvent was removed by rotary evaporation at reduced pressure to give a light-yellow solid as crude product. The crude product was recrystallized using 5 mL of a hexane/ethanol mixture (10:1) and then air dried to give **26** as a white solid (0.11 g, 72%). M.p. 153.5-154.0 °C. ^{1}H NMR (500 MHz, CDCl$_3$) δ 7.76 – 7.70 (m, 4H), 7.53 (dd, *J* = 3.0, 5.3 Hz, 2H), 7.50 – 7.40 (m, 6H), 7.15 (dd, *J* = 3.0, 5.3 Hz, 2H), 3.68 (s, 6H). ^{13}C NMR (126 MHz, CDCl$_3$) δ 164.14, 153.90, 149.13, 133.16, 129.08, 128.58, 128.00, 125.99, 122.20, 94.05, 52.29. UV-Vis λ_{max} (1×10^{-4} M in CH$_2$Cl$_2$) 230 nm. HRMS (ESI): 381.1115 [calc'd for M$^+$ - OCH$_3$: 381.1127].

Dimethyl 1,4-dimesityl-1,4-dihydro-1,4-epoxynaphthalene-2,3-dicarboxylate (**27**):

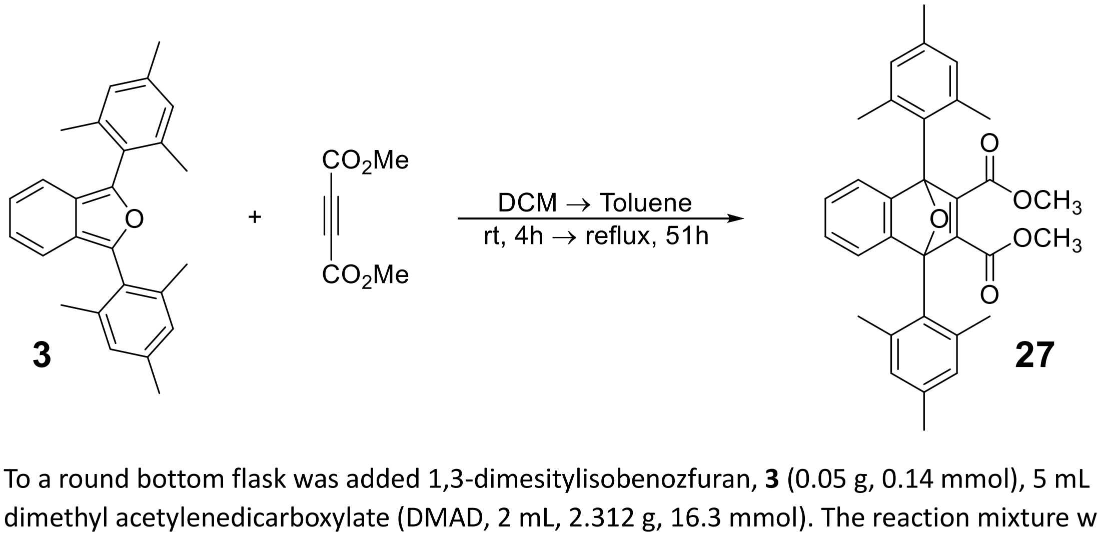

To a round bottom flask was added 1,3-dimesitylisobenozfuran, **3** (0.05 g, 0.14 mmol), 5 mL CH$_2$Cl$_2$ and dimethyl acetylenedicarboxylate (DMAD, 2 mL, 2.312 g, 16.3 mmol). The reaction mixture was stirred at room temperature for 4 hours. The solvent was removed by rotary evaporation at reduced pressure to give a light-yellow solid. A TLC (hexane: EtOAc = 3:1) indicated no reaction. Additional DMAD was added to the unreacted mixture in the round bottom flask (2 mL, 2.312g, 16.3 mmol) along with 2 mL toluene. After attaching a reflux condenser, the mixture was heated to reflux for 51 hours. The mixture was cooled to room temperature and toluene was removed by rotary evaporation at reduced pressure to give a sticky, dark brown solid. The solid was pre-purified by silica gel CombiFlash chromatography (hexane/EtOAc = 9/1) to obtain a yellow oil as crude product (23 mg). Finally, the crude product was purified by preparative TLC (petroleum ether/EtOAc = 3:1) to give **27** as a yellow powdery solid (15 mg, 22%, 35% based on reacted **3**). M.p. 180 °C (decomp.). ^{1}H NMR (700 MHz, $CDCl_3$) δ 7.29 (dd, *J* = 3.0, 5.3 Hz, 2H), 6.98 (dd, *J* = 3.0, 5.3 Hz, 2H), 6.88 (s, 4H), 3.64 (s, 6H), 2.30 (s, 12H), 2.28 (s, 6H). ^{13}C NMR (176 MHz, $CDCl_3$) δ 164.38, 155.13, 151.10, 139.03, 137.93, 130.68, 128.02, 124.72, 124.49, 95.54, 51.98, 23.71, 20.75. HRMS (ESI): 497.2316 [calc'd for $M+H^+$: 497.2328].

Acknowledgements

The authors gratefully acknowledge financial support from the University of New Hampshire

References

---

[1] Clar, E. *The Aromatic Sextet, Pp. 12-16*; J. Wiley, **1972**.

[2] P. v. R. Schleyer, M. Manoharan, H. Jiao, F. Stahl. The Acenes: Is There a Relationship between Aromatic Stabilization and Reactivity? *Org. Lett.* **2001**, *3*, (23), 3643–3646. https://doi.org/10.1021/ol016553b

[3] Matsuoka, S.; Jung, S.; Miyakawa, K.; Chuda, Y.; Sugimoto, R.; Hamura, T. Didehydroisobenzofuran: A New Reactive Intermediate for Construction of Isoacenofuran. *Chem. – Eur. J.* **2018**, *24* (71), 18886–18889. https://doi.org/10.1002/chem.201804655

[4] Kitamura, K.; Kudo, R.; Sugiyama, H.; Uekusa, H.; Hamura, T. Isoacenofuran: A Novel Quinoidal Building Block for Efficient Access to High-Ordered Polyacene Derivatives. *Chem. Commun.* **2020**, *56* (95), 14988–14991. https://doi.org/10.1039/D0CC06620F.

[5] Kaur, I.; Jia, W.; Kopreski, R. P.; Selvarasah, S.; Dokmeci, M. R.; Pramanik, C.; McGruer, N. E.; Miller, G. P. Substituent Effects in Pentacenes: Gaining Control over HOMO−LUMO Gaps and Photooxidative Resistances. *J. Am. Chem. Soc.* **2008**, *130* (48), 16274–16286. https://doi.org/10.1021/ja804515y.

---

[6] Kaur, I.; Stein, N. N.; Kopreski, R. P.; Miller, G. P. Exploiting Substituent Effects for the Synthesis of a Photooxidatively Resistant Heptacene Derivative. *J. Am. Chem. Soc.* **2009**, *131* (10), 3424–3425. https://doi.org/10.1021/ja808881x.

[7] Kaur, I.; Jazdzyk, M.; Stein, N. N.; Prusevich, P.; Miller, G. P. Design, Synthesis, and Characterization of a Persistent Nonacene Derivative. *J. Am. Chem. Soc.* **2010**, *132* (4), 1261–1263. https://doi.org/10.1021/ja9095472.

[8] Blicke, F. F.; Patelski, R. A. A Further Study of 2-(4″-Hydroxybenzoyl)-4’-Hydroxybenzophenone1. *J. Am. Chem. Soc.* **1936**, *58* (2), 273–276. https://doi.org/10.1021/ja01293a023.

[9] Spartan ’20, Wavefunction, Inc., Irvine, CA; Y. Shao et al., *Mol. Phys.* **2015**, *113* (2), 184–215. https://doi.org/10.1080/00268976.2014.952696.

[10] Cava, M. P.; Mitchell, M. J.; Deana, A. A. Condensed Cyclobutane Aromatic Compounds. XIII. An Attempted Synthesis of 1,2-Diphenylbenzocyclobutene. *J. Org. Chem.* **1960**, *25* (9), 1481–1484. https://doi.org/10.1021/jo01079a005.

Nishina, Y.; Kida, T.; Ureshino, T. Facile Sc(OTf)3-Catalyzed Generation and Successive Aromatization of Isobenzofuran from o-Dicarbonylbenzenes. *Org. Lett.* **2011**, *13* (15), 3960–3963. https://doi.org/10.1021/ol201479p.

[11] Gaussian 09, Revision E.01, M. J. Frisch, G. W. Trucks, H. B. Schlegel, G. E. Scuseria, M. A. Robb, J. R. Cheeseman, G. Scalmani, V. Barone, B. Mennucci, G. A. Petersson, H. Nakatsuji, M. Caricato, X. Li, H. P. Hratchian, A. F. Izmaylov, J. Bloino, G. Zheng, J. L. Sonnenberg, M. Hada, M. Ehara, K. Toyota, R. Fukuda, J. Hasegawa, M. Ishida, T. Nakajima, Y. Honda, O. Kitao, H. Nakai, T. Vreven, J. A. Montgomery, Jr., J. E. Peralta, F. Ogliaro, M. Bearpark, J. J. Heyd, E. Brothers, K. N. Kudin, V. N. Staroverov, T. Keith, R. Kobayashi, J. Normand, K. Raghavachari, A. Rendell, J. C. Burant, S. S. Iyengar, J. Tomasi, M. Cossi, N. Rega, J. M. Millam, M. Klene, J. E. Knox, J. B. Cross, V. Bakken, C. Adamo, J. Jaramillo, R. Gomperts, R. E. Stratmann, O. Yazyev, A. J. Austin, R. Cammi, C. Pomelli, J. W. Ochterski, R. L. Martin, K. Morokuma, V. G. Zakrzewski, G. A. Voth, P. Salvador, J. J. Dannenberg, S. Dapprich, A. D. Daniels, O. Farkas, J. B. Foresman, J. V. Ortiz, J. Cioslowski, and D. J. Fox, Gaussian, Inc., Wallingford CT, 2013.